Fragmentation and energy loss in grazing scattering of copper clusters Cu_n from a single-crystal Al(111) surface

Xianwen Luo,* Bitao Hu,† and Chengjun Zhang
School of Nuclear Science and Technology, Lanzhou University, Lanzhou 730000, China
(Received 18 August 2011; revised manuscript received 16 January 2012; published 19 April 2012; corrected 16 July 2012)

By performing a molecular dynamics simulation, fragmentation and energy losses of neutral copper clusters Cu_n in grazing incidence on a single-crystal Al(111) surface under various azimuthal angles were studied. The interactions among copper atoms were modeled by tight-binding potential, and the position of each copper atom at each time step was calculated by integrating the Newton equations of motion. The percentage of unfragmented clusters as a function of incident energies, incident angles, and cluster sizes was found to be almost independent of the influence of surface structure. The regular-sized clusters without icosahedral structure appear to be less stable. The energy spectra of reflected particles for 30-keV copper clusters Cu_{147} grazing scattering were measured under three incident angles, and some additional peaks appearing on the left side of the first peak were observed for large grazing angles of incidence.

DOI: 10.1103/PhysRevA.85.043201 PACS number(s): 36.40.Qv, 34.50.Bw, 61.85.+p

I. INTRODUCTION

Owing to their specific mechanical, electronic, catalytic, and magnetic properties, clusters have attracted much attention in the past decade [1–5], and recently, in particular, metal clusters are expected to be highly important in a variety of applied processes, such as deposition, growth of high-quality ultrathin films without damaging the substrate surface geometry, and creating nanoscale materials [6,7]. One important way to study cluster is to scatter it from an insulator or metal surface under a grazing angle of incidence. In the majority of cases cluster-surface interactions accompanied by inelastic processes, such as excitation of cluster and electronic energy loss, can be favorably studied using channeling effect [8,9]. When a cluster reaches a metal surface under grazing incidence, it would not penetrate into the surface, but reflect specularly from the surface without destruction of its geometry or dissociating into small fragments. Therefore, information on the stability of clusters, even the fragmentation pattern, can be obtained by looking at the outgoing fragments.

From former available studies performed with projectile energies of typically hundreds of eV to some keV, and a large angle to grazing impact, details on the fragmentation of clusters [10,11] and kinetic energy loss [10,12] were widely revealed. In order to investigate the fragmentation of clusters, four sizes of fullerenes were used as projectiles in previous surface-impact research, and the fragmentation of the four sizes of fullerenes impacting on the surface as a function of impact energy per carbon atom was shown by Chancey *et al.* [11]. However, most of these studies, e.g., studies performed in Refs. [7,13], did not pay attention to the influence of the target, especially the target with a detailed description of surface structure. The clusters have been proved to be easily dissociated into fragments during cluster–ion-surface collisions. When clusters are used as projectiles, interesting aspects may arise with respect to fragmentation phenomena, as compared to single atomic or ionic projectiles.

Furthermore, information on the stability of various clusters also can be obtained by measuring the energy loss of projectiles, which is traditionally divided into two components of nuclear stopping and electronic stopping. The energy losses of H_2^+ and H_3^+ ions passing through carbon foils without fragmentation were reported by Susuki *et al.* [12], and the energy losses were well explained in terms of electronic stopping power. Although both nuclear and electronic energy losses are expected to be almost completely suppressed under grazing scattering, rather large energy losses of C_{60}^+ ions grazing scattering from an insulator surface under three different angles of incidence were still observed [13]. The anomalous energy losses were attributed to the internal excitations, which cause the observed fragmentation of C_{60}^+ ions. Nevertheless, the fragmentation of C_{60}^+ ions occurs for energy-loss measurement in all cases, leading to the ambiguous evidence on the existence of critical impact energy of fragmentation.

Motivated by these previous studies, we go further by using larger copper clusters Cu_n with energies ranging from some keV to thousands of keV grazing scattering from a single-crystal Al(111) surface. The copper clusters were modeled as the collections of the point atoms subjected to the tight-binding interaction potential. The percentage of clusters that remain unfragmented was measured as a function of incident energies, incident angles, and different investigated cluster sizes. Furthermore, the energy losses of copper cluster Cu_{147} grazing scattering from crystal surface were measured under different conditions, producing no fragmentation or intensive atomization of the cluster. The organization of the paper is as follows. In the following sections, the simulation models including the motion of clusters, fragmentation determination, and energy loss are presented, and then the calculation results are discussed. A short conclusion can be found in Sec. IV.

II. MODELING

Motivated by grazing ion-surface scattering, the trajectories of an atom "*i*" in a copper cluster are predominantly

*Present address: UPMC Sorbonne Universités, CNRS-UMR7588, Institut des NanoSciences de Paris, F-75005, Paris, France.
†Corresponding author: hubt@lzu.edu.cn

determined by the interatomic interaction potential between the atom i and the lattice atoms. In addition, its trajectories are also affected by the interactions among copper atoms. In the present study, the second moment tight-binding approximation (TB-SMA) was employed for the description of Cu-Cu interatomic interactions [14,15]. Previous works have proved that the TB-SMA potential is accurate and convenient in the description of interatomic interactions [4,16,17]. Therefore, for an atom i among copper clusters at a distance R away from the crystal surface, the position of this atom at each time step is subjected to two forces:

$$\vec{F}_i(R) = \sum_{i \neq j} \vec{F}(r_{ij}) + \sum \vec{F}_{\mathrm{TFM}}(R), \tag{1}$$

where the first item is the sum of interatomic Cu-Cu forces depending on the potential energy of the atom i. For the atom i, the total potential energy, which is composed of two components written as E_b^i and E_r^i, respectively, is given by the following equations:

$$\begin{aligned} E_{\mathrm{coh}} &= \sum_{i \neq j} \left(E_b^i + E_r^i\right), \\ E_b^i &= -\left\{\sum_{i \neq j} \xi^2 \exp\left[-2q\left(\frac{r_{ij}}{r_0} - 1\right)\right]\right\}^{1/2}, \\ E_r^i &= \sum_{i \neq j} A \exp\left[-p\left(\frac{r_{ij}}{r_0} - 1\right)\right], \end{aligned} \tag{2}$$

where E_b^i is an attractive energy; E_r^i is the repulsive energy which is described by a pair potential energy of the Born-Mayer form; r_{ij} represents the distance between atoms i and j; r_0 is the first-neighbor distance in a copper cluster; ξ is an effective hopping integral and q describes its dependence on the relative interatomic distance; and p is related to the compressibility of bulk metal. These potential parameters associated with Cu-Cu atoms were given in Ref. [18].

The second term in Eq. (1) is the sum of the forces experienced by the atom i in a copper cluster from all target atoms. Correspondingly, the force experienced by the atom i from a target atom can be given by

$$\vec{F}_{\mathrm{TFM}}(R) = \frac{d}{dR}[W_{\mathrm{TFM}}(R)], \tag{3}$$

where the $W_{\mathrm{TFM}}(R)$ is the Coulomb potential between the atom i and a target atom. The interaction potential for atomic species with atomic numbers Z_1 and Z_2 separated by a distance r can be approximated by a screened Coulomb potential of this type:

$$W_{\mathrm{TFM}} = \frac{Z_1 Z_2}{r} \phi(r/a_F), \tag{4}$$

where $\phi(r/a_F)$ is an interatomic "screening function." In our simulation, we adopted the Thomas-Fermi-Moliere screening function as follows:

$$\phi(r/a_F) = \sum_i a_i \exp(-b_i r/a_F), \tag{5}$$

in which $a_i = \{0.35,0.55,0.1\}$, $b_i = \{0.3,1.2,6.0\}$, and the screening length

$$a_F = \frac{0.8854}{\sqrt{Z_1^{2/3} + Z_2^{2/3}}}. \tag{6}$$

In order to simplify the calculation, when the copper atom i-surface distances $R > 5.0$ a.u., the interaction potential between the copper atom i and target atoms is approximated by a continuum potential [19]

$$\sum W_{\mathrm{TFM}}(R) = 2\pi n_s Z_1 Z_2 a_F \sum_i \frac{a_i}{b_i} \exp(-b_i R/a_F), \tag{7}$$

where n_s is the number of surface atoms per unit area. According to Eq. (7), the continuum potential depends only on the distance R normal to the surface plane.

The structure and stability of Cu_n clusters consisting of 10–10 000 atoms are sensitive to the number of atoms. In the present work, the so-called magic-numbered clusters [20,21], which are based on icosahedral geometry, were mainly adopted as projectiles. The number of atoms in a magic-sized Cu_n can be obtained by the relationship $N_k = (10k^3 + 15k^2 + 11k + 3)/3$, with N_k being the number of atoms and k the layers of the icosahedral clusters. Such clusters have been found for $N_k = 13,55,147,309,561, \ldots$ corresponding to the formation of the first, the second, the third, the fourth, and the fifth Mackay icosahedral [21]. The icosahedral cluster growth pattern is generally multilayered icosahedral or layer by layer growth, from the one-shell Mackey icosahedral Cu_{13} to the two-shell icosahedral Cu_{55} and then to the 147-atom structure, which is the third Mackey icosahedron [21]. Moreover, the random-sized Cu_n clusters can be derived from the already known one with $n - 1/n + 1$ atoms by simply adding or removing one atom.

At the beginning of each event, the copper clusters were initially placed at a sufficiently large distance above the crystal surface, and therefore the Coulomb interaction potential between the cluster and the lattice atoms could be ignored. Thus, if the copper cluster is outside the range of Coulomb potential, it remains in its static equilibrium geometry with all atoms assigned a uniform velocity to the surface and consistent with the desired incident energy. The present work used a single-crystal aluminum target with a clean and flat surface, in which the surface channels were displayed along the directions of $[1,0,\bar{1}]$ and $[0,1,\bar{1}]$, etc., presented in Fig. 1. The origin coordinate system was put at the center of the crystal surface (the intersection of lines with arrow) with the x and y axes parallel to the surface and the z axis perpendicular to the surface. According to the Debye model, thermal vibrations were included by calculating random displacements of the target atoms with the surface Debye temperature, and the Debye temperature of 390 K was taken for two dimensions of the surface plane.

Compared with the size of incident Cu_{147} clusters, the target normally used in experiment, e.g., a sample with the size of 8×10 mm^2, is far larger and consequently seems to have infinite surface area. Thus, a target with infinite surface plane is needed in the present molecular dynamics (MD) simulation. At the very beginning, based on the single-crystal

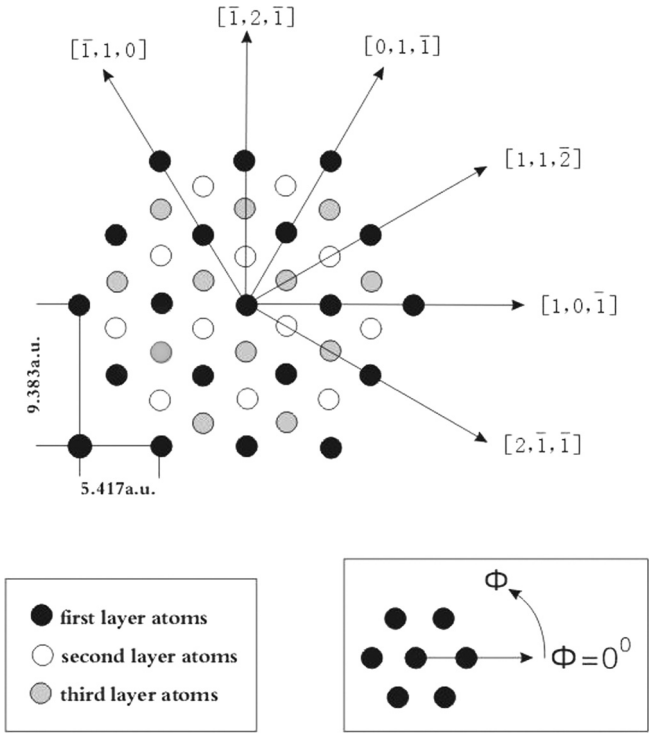

FIG. 1. The schematic diagram of single-crystal Al(111) surface structure.

Al(111) surface structure displayed in Fig. 1, a large target consisting of 2307 atoms distributed evenly in three layers was generated, and its size was much larger than that of copper clusters, even if the Cu_{1415} clusters were used as projectiles. A schematic diagram for copper cluster grazing scattering is shown in Fig. 2 by applying the target with all 2307 atoms. However, the consumption of computer resources is enormous when cluster-surface distances $R < 5.0$ a.u., because all target atoms will be involved in the calculation of the interaction potential between the copper atom i and target atoms at each time step. Actually, the calculation of the interaction potential between the copper atom i and the crystal surface can be well approximated by considering only the nearest 75 target atoms.

Generally, the target with 2307 atoms was only used for two purposes: (i) obtaining the schematic diagram of copper cluster grazing scattering and (ii) providing the coordination noted as $x_{\rm mid}(i)$ and $y_{\rm mid}(i)$ of the target atom which is closest to the copper atom i. Therefore, during Cu_n cluster grazing scattering, n targets, i.e., target (1), target (2), ... target (i), ... target (n), consisting of 75 atoms were generated and their coordinate system centers were put exactly on $x_{\rm mid}(i)$ and $y_{\rm mid}(i)$. Then, the position of target (i) along the surface dimension of x,y directions is adjusted frequently as if the copper atom i interacts with an infinite surface plane. This technology was used in our previous work [22] and will be described in detail in our future paper. By using this method, the simulation of large copper clusters interacting with virtual infinite surface can be performed within an acceptable computation time.

The characteristics of incident cluster beams, such as energy spectra and angular distribution, etc., were modeled as a Gaussian line shape. In addition, the interaction interface was described as a vacuum-surrounded area to meet the real experimental conditions as much as possible. Based on the fact that the tight-binding (TB) potential has a finite distance cutoff, a fragment was defined as a group of atoms, each of which has a nonzero interaction with some other members of the group, and the fragmentation of the copper cluster was determined from the atomic positions at the end of simulation. By using the above modeling and time step of 1 a.u., the copper cluster's motion was simulated by a stepwise integration of the Newton equations of motion. Fragmentation statistics or energy losses at each time were analyzed from sets of 1000 trajectories. The process including trajectory calculation and fragment determination was carried out using a molecular dynamics program developed by our group. The running time of each simulated event was 5 ps, covering both the collision and the relaxation phases.

The energy loss that copper atom i experiences along its trajectory can be interpreted as a sum of two components: (i) elastic energy loss and (ii) inelastic energy loss.

Elastic energy loss. The elastic energy loss can be easily calculated from the binary collisions between copper atoms and lattice atoms as follows [23]:

$$\Delta E_{\rm el} = E_0\left[1-\left(\frac{\cos\theta \pm \sqrt{(\mu^2-\sin^2\theta)}}{1+\mu}\right)^2\right], \qquad (8)$$

where E_0 denotes the initial kinetic energy of projectiles, θ is the scattering angle, and $\mu = m_t/m_p$ (m_t and m_p are the mass of projectiles and lattice atoms). The plus sign is applied for $m_p \leqslant m_t$, otherwise, the minus sign is chosen.

Inelastic energy loss. In our previous work [22], the inelastic energy loss coming from three sources for highly charged ion (HCI) grazing on metallic surface was discussed. Since neutral copper clusters are used as projectiles in the present work, only when the cluster is close enough to reach electron gas of the metallic surface ($R \leqslant 5.0$ a.u), the electron energy-loss process begins and its values can be obtained by integrating the position-dependent stopping power [24]

$$S_e(R) = 2k_F^2\frac{v}{v_F}\int_0^1 kdk[\sigma_n(k)]^2 H(k,z_0'), \qquad (9)$$

where R is the distance from the top surface layer, $z_0' = R - r_d$, $r_d = 2.99$ a.u. is the average atomic radius of the aluminum target, and $k_F = v_F$ is the Fermi wave number. According to the Brandt-Kitagawa (BK) model [25],

$$\sigma_n(k) = Z_1\frac{q(R)+(2kk_F\Lambda)^2}{1+(2kk_F\Lambda)^2}, \qquad (10)$$

where Z_1 is the atomic number of projectiles, Λ is a screening length, and $q(R)$ is the position-dependent ionization degree. When $R > r_d$, the position-dependent ionization degree can be expressed as

$$q(R) = q_0\exp\left[-\exp\left(-\frac{R-z_s}{L}\right)\right], \qquad (11)$$

where q_0 is the initial ionization degree and L is a characteristic length, $z_s = L\ln(\Gamma_0 L/v_n)$ with v_n being the perpendicular velocity and Γ_0 a typical resonant ionization rate, but for $R < r_d$, an empirical model based on the velocity-dependent

electron-stripping criterion in which the ionization degree shows a good agreement with experiment values for heavy ions is adopted as

$$q_b = 1 - \exp\left(0.803 y_r^{0.3} - 1.3167 y_r^{0.6} - 0.381\,57 y_r - 0.008\,983 y_r^2\right), \quad (12)$$

where $y_r = v_r / Z_1^{2/3}$, with v_r being the ion velocity relative to the target-electron velocity, as defined in Ref. [24]. In Eq. (9), the detailed expressions for $H(k, z_0')$ was given in Refs. [24,26]. The electron energy loss dE experienced by copper atom i moving dL distance is calculated as follows:

$$dE = S_e(R) dL, \quad (13)$$

where $S_e(R)$ characterizes the position-dependent stopping power, dL is the effective ion–atom-surface interaction length, i.e., the part of the trajectory in which copper atom i interacts efficiently with surface electron gas. Because the electron-energy-loss process is switched on only when the copper atom i is close enough to the metallic surface, the effective trajectory length is computed only when $R \leqslant 5.0$ a.u.

III. RESULTS AND DISCUSSION

Figure 2 shows a schematic diagram from copper clusters grazing on a single-crystal Al(111) surface under a random azimuthal angle with respect to the $[1,0,\bar{1}]$ direction of the target surface. Interatomic interaction potentials between copper clusters and surface atoms lead to the forces normal to the surface, introducing the reflection of copper atoms. The snapshots shown below for Cu_{147} cluster grazing scattering are taken at the distance of 20 a.u. away from the surface in the collision phase, the distances of closest approach, and the distance of 20 a.u. away from the surface in the relaxation phase, respectively. For the case of the upper one of Fig. 2, even though the incident energy is far larger than the binding energies of individual atoms, e.g., the incident energy of Cu_{147} clusters is 30 keV, which is far larger than the binding energy per atom of the 3.388 eV/atom, the Cu_{147} clusters could still be reflected from the surface without destruction of its icosahedral structure, and therefore no fragmentation takes place. However, fragmentation of Cu_{147} clusters will take place at higher incident energy, shown in the bottom one of Fig. 2, indicating the existence of a critical energy at which the copper clusters Cu_{147} begin to shatter into a number of fragments.

One way to characterize the stability of clusters grazing on a surface is to measure the percentage of clusters that remain unfragmented at the final step of the simulation. The number of copper atoms in the original incidence clusters is denoted as N_0. Then, the percentage of copper clusters that remain unfragmented can be obtained by N_f/N_0, where N_f stands for the number of atoms in the largest fragment at the end of grazing scattering. It should be noted that this largest fragment, which is able to be considered as the reflected particle, is the specific one preserving the properties of the original incident clusters as much as possible. If the Cu_{147} copper clusters would be reflected from the surface without fragmentation, N_f is equal to the parameter N_0. As a result, the percentage of copper clusters that remain unfragmented will be equal to 1.

Figure 3(a) shows the percentage of clusters that remain unfragmented as a function of incidence energy. For sufficiently small incident energies, the copper clusters will be specularly reflected from the surface without fragmentation and the corresponding percentage of clusters that remain unfragmented will be equal to 1. In contrast, with the increase of incident energies, the copper cluster appears to be less stable when the incident energies are larger than a critical value ~47 keV. Then, fragmentation occurs and the percentage of unfragmented clusters decreases dramatically with the increase of incident energy. As shown in Fig. 3(b), the fragmentation yield obtained by $1 - N_f/N_0$ suddenly increases at incident energies slightly larger than the critical energy.

Three different azimuthal angles with respect to the low-index $[1,0,\bar{1}]$ direction of the Al(111) surface were adopted to observe whether or not the surface structure has an influence on fragmentation outcomes. Inspired by ion–atom-surface grazing [22], it is reasonable to believe that if the azimuthal angle of the plane of incidence coincides with a low-index direction on the crystal surface plane, grazing can occur along strings of surface atoms in the regime of "axial channeling." For instance, axial channeling happens when copper clusters graze under azimuthal angles of $\Phi = 0^\circ$ or $\Phi = 60^\circ$. Otherwise, "planar channeling" happens if the clusters graze along random directions, e.g., under azimuthal angle $\Phi = 10^\circ$. According to the present results, the percentage of clusters that remain unfragmented almost has no change when cluster

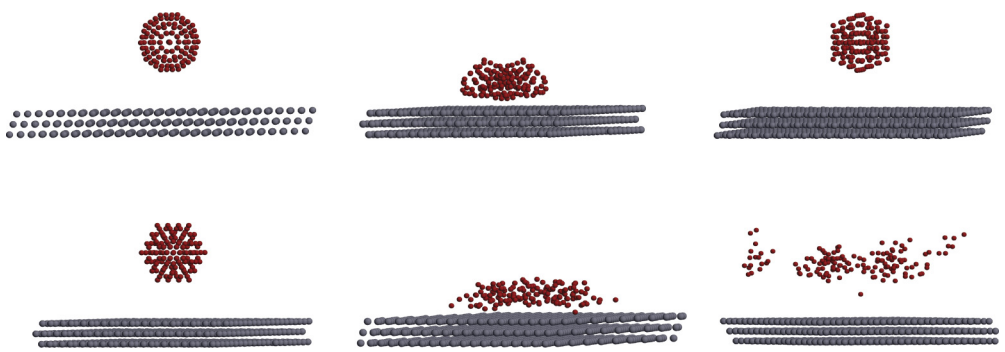

FIG. 2. (Color online) Simulated fragmentation collisions of copper clusters Cu_{147} grazing under the incidence angle $\theta_{in} = 3^\circ$ on a single-crystal Al(111) surface at the incident energies of 30 (upper) and 80 keV (bottom). From left to right: before, during, and after grazing on an Al(111) surface.

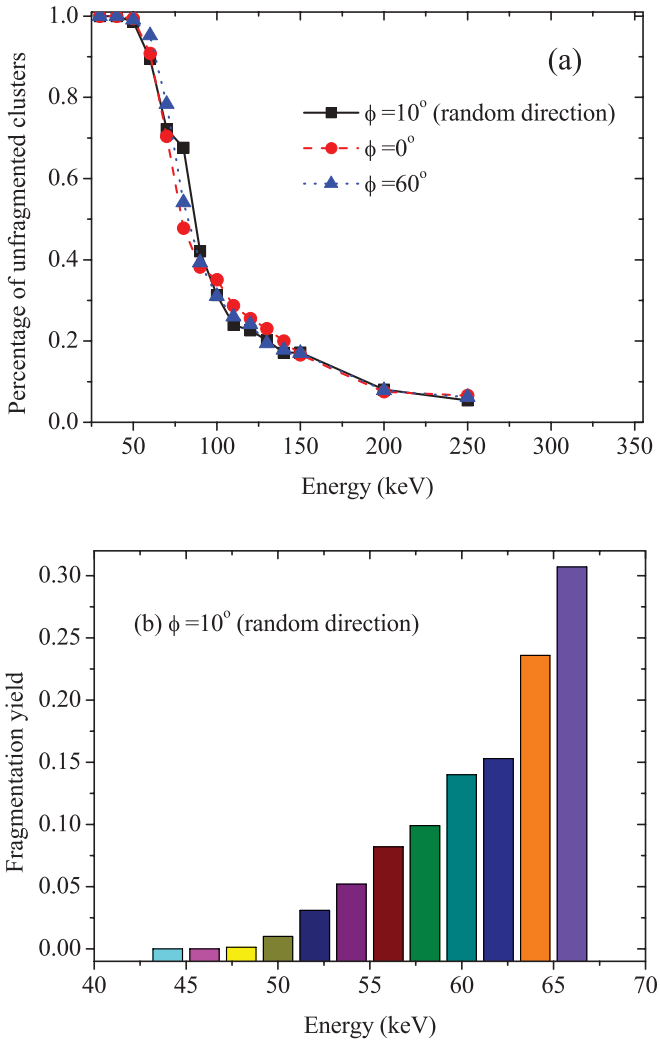

FIG. 3. (Color online) (a) Percentage of clusters that remain unfragmented as a function of incident energy for Cu_{147} clusters grazing on the Al(111) surface under a grazing angle of incidence $\theta_{in} = 3°$. The azimuthal angles of incident beams with respect to the low-index ($[1,0,\bar{1}]$) direction are chosen as $\Phi = 10°$, $\Phi = 0°$, and $\Phi = 60°$. (b) Fragmentation yield around incident energy $E = 47$ keV. The lines are drawn to guide the eyes.

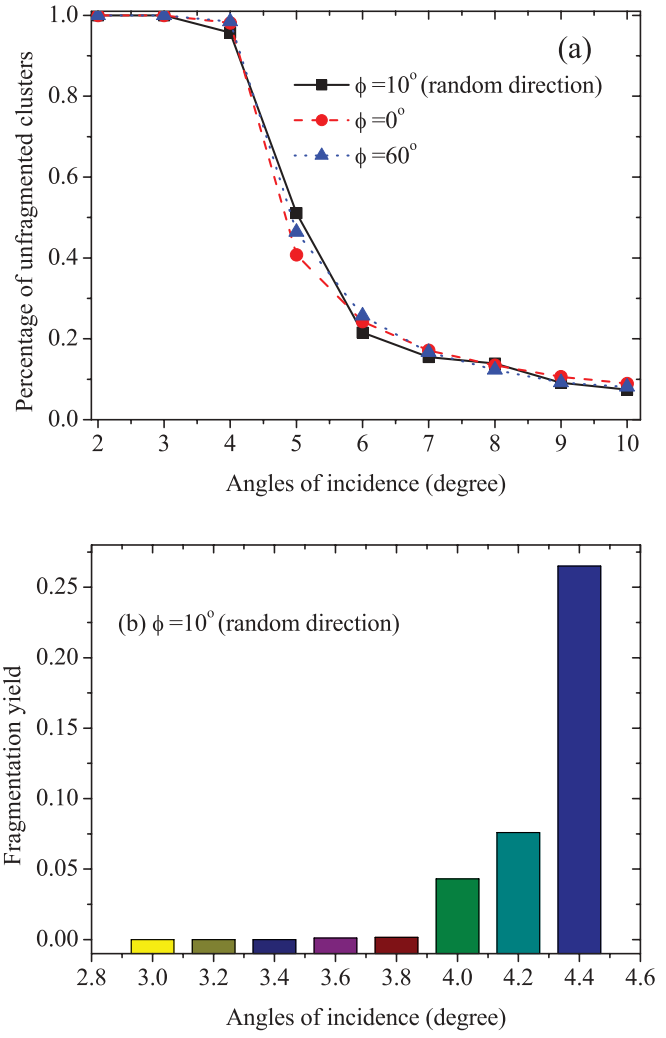

FIG. 4. (Color online) (a) Percentage of clusters that remain unfragmented as a function of angles of incidence for 30 keV Cu_{147} clusters grazing on an Al(111) surface. The azimuthal angles of incident beams with respect to the low-index ($[1,0,\bar{1}]$) direction also are chosen as $\Phi = 10°$, $\Phi = 0°$, and $\Phi = 60°$. (b) Fragmentation yield around the angle of incidence $\theta_{in} = 3.8°$. The lines are drawn to guide the eyes.

beams are changed from planar to axial surface grazing scattering.

As shown in Fig. 4(a), the percentage of clusters that remain unfragmented decreases dramatically when the incident angles θ_{in} are larger than the critical value $\theta_{in} = \sim 3.8°$. For sufficiently small incident angles, the clusters are reflected from the crystal surface without destruction of its geometry, and therefore no fragmentation takes place. In Fig. 4(b), the fragmentation yield suddenly increases when the angles of incidence are slightly larger than the critical value, which is similar to the tendency shown in Fig. 3(b). Reference [11] reported that the threshold impact energy of ~2.5 eV/atom does exist for C_{60} impacting on a structureless wall. However, the fragmentation of C_{60}^+ ions occurs via a sequential C_2-loss process for energy-loss measurement [13], even if the perpendicular energy is far smaller than the threshold impact energy. From the present results, the critical energy of the fragmentation of Cu_{147} clusters does exist under grazing scattering condition.

In Ref. [13], the effect of internal excitation was investigated experimentally for the insulator target under suppressing nuclear and electronic stopping, which can be achieved by using grazing scattering geometry. In order to estimate the internal energy of the scattered fullerenes, simulations of fragment spectra using an Arrhenius representation of rates for delayed C_2 loss and electron emission for parameters from Concina *et al.* [29] had been performed [30,31]. Their simulations reproduce the trends generally but underestimate the internal excitation, especially for small angles of incidence. In the present work, copper clusters were modeled as collections of point atoms subject to the TB potential, so that the description of the electronic system of projectiles was not accurate enough. Then, the study of the internal excitation of scattered clusters is beyond reach.

According to $E_\perp = E_0^* \sin^2(\theta_{in})$, the defined vertical energy $E_\perp$ were achieved by combining the incident angles θ_{in} and initial incident energies E_0. Accordingly, the vertical energy $E_\perp$ normal with respect to the surface always increases with the increase of incidence angle θ_{in} or initial incident energies E_0. For the above two cases of Figs. 3(b) and 4(b), the vertical energies at which incident Cu_{147} clusters begin to shatter are 128.8 and 131.7 eV, respectively. For Cu_n clusters with greater vertical energies, the distances of closest approach are closer to the crystal surface, and consequently the surface potential has a greater influence on the incident clusters and leads to more intensive fragmentation.

In the previous work [22], we showed that the surface structure has a great influence on SHCI (slow highly charged ion)-surface interaction due to the fact that the effective trajectory length can be prolonged by the axial channeling along the very axis (low-index directions). However, as shown in Figs. 3(a) and 4(a), the surface structure almost has no effect on the fragmentation outcomes for copper clusters Cu_{147} grazing on the Al(111) surface.

Two facts would be expected to be responsible for the differences between HCI and cluster grazing scattering from the surface. (i) The influence of channeling effect is not obvious when the projectiles are far away from the surface. For instance, if the distance of closest approach is larger than 3 a.u. for the neutral Ar^0 atom grazing on the Al(111) surface, the closest approach distance would not change significantly when incident beams are changed from planar to axial surface scattering. (ii) When the copper atom i is not close enough to the surface, other atoms in this Cu_{147} cluster make more of a contribution to the motion of copper atom i than the target atoms. For incident angle $\theta_{in} = 10^\circ$, the distances of closest approach for Cu_{147} clusters grazing under $\Phi = 10^\circ$, $\Phi = 0^\circ$, and $\Phi = 60^\circ$ are ~3.04, ~3.06, and ~3.04 a.u., respectively, and therefore there is almost no influence from surface structure. These results indicate that the stability of clusters impacting or grazing on surface can be studied by simply adjusting the incident angles or energies without having to consider the influence of the surface structure on fragmentation outcomes. On the other hand, for large angles of incidence, fragmentation of incident clusters with large vertical energy $E_\perp$ is intensive no matter which direction the clusters would initially graze along. This phenomenon indicates that it is inappropriate to detect the information on surface structure by looking at the fragmentation outcomes for cluster grazing scattering from crystal surface.

Figure 5 shows the percentage of four sizes of clusters that remain unfragmented as a function of the incident energy per atom. As is seen above, the clusters with icosahedral structure, such as Cu_{147}, Cu_{561}, and Cu_{1415} clusters, appear more stable with respect to fragmentation outcomes than regular-sized cluster Cu_{100}. Nevertheless, the tendency of Cu_{100} fragmentation is similar to that of the other investigated clusters. Moreover, from the present results, the percentage of clusters that remain unfragmented is not equal to 0 at high incident energies range. For instance, the unfragmented percentage is not equal to 0 even when the cluster is at full atomization, e.g., ~1/147 for full atomization. This feature is greatly different from the results of Chancey *et al.* [11], in which they did not show clearly the way to define the

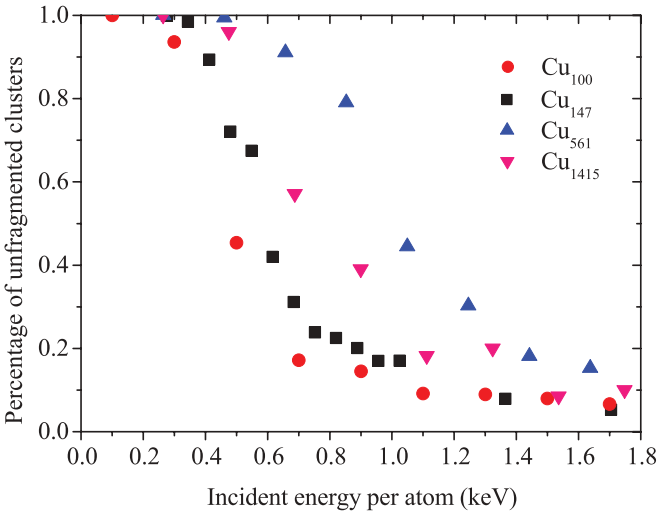

FIG. 5. (Color online) Percentage of clusters that remain unfragmented as a function of the incident energy per atom for Cu_{100}, Cu_{147}, Cu_{561}, and Cu_{1415} clusters grazing on an Al(111) surface under the incidence angle of $\theta_{in} = 3^\circ$.

parameter of unfragmented percentage. On the other hand, if larger clusters are used as projectiles, the opportunities of the recombination of outgoing small fragments into bigger ones is greater in the relaxation phase, and therefore there are more atoms in the largest fragment.

Based on the results from Fig. 4(a), two incidence angles of $\theta_{in} = 4^\circ$, 5° at which any fragmentation occurs but without leading to full atomization of Cu_n clusters were adopted to observe the distribution of fragmentation outcomes. The fragment distributions from the grazing scattering of Cu_{147} clusters on the Al(111) surface are shown in Fig. 6. The raw data are displayed directly about the total number of fragmentation outcomes in each size, providing the advantage of showing an intuitive and clear status of fragments. From Fig. 6(a), the fragment distribution appears symmetric between the small and large fragments. However, the fragment distribution shown in Fig. 6(b) ceases to be symmetric and the intensity of large fragments decreases down to almost 0, indicating the clusters undergo further fragmentation compared to that in Fig. 6(a). The vertical energy $E_\perp$ for clusters Cu_{147} grazing under angles of incidence $\theta_{in} = 4^\circ$,5° is about 145.98 and 227.88 eV, respectively. As evident from Fig. 6, the result is consistent with the fact that the appearance of fragment distribution depends significantly upon the vertical energy $E_\perp$, and greater vertical energy $E_\perp$ leads to more intensive fragmentation.

If copper clusters Cu_{147} are used as projectiles, the energy-loss processes begin only when projectiles are close enough to the metallic surface so that the electron energy-loss process can switch on. Since the diameter of Cu_{147}, ~30 a.u. is much larger than the average aluminum atomic radius r_d of 2.99 a.u., when a group of atoms in a Cu_{147} cluster is close enough to the metal surface, other groups of atoms are still out of the range of surface electron gas. In this case, only the former group of atoms makes a contribution to the electronic stopping. Furthermore, elastic energy loss which results from energy transfer in elastic binary collisions from projectiles to lattice atoms may play a different role in cluster-surface collisions.

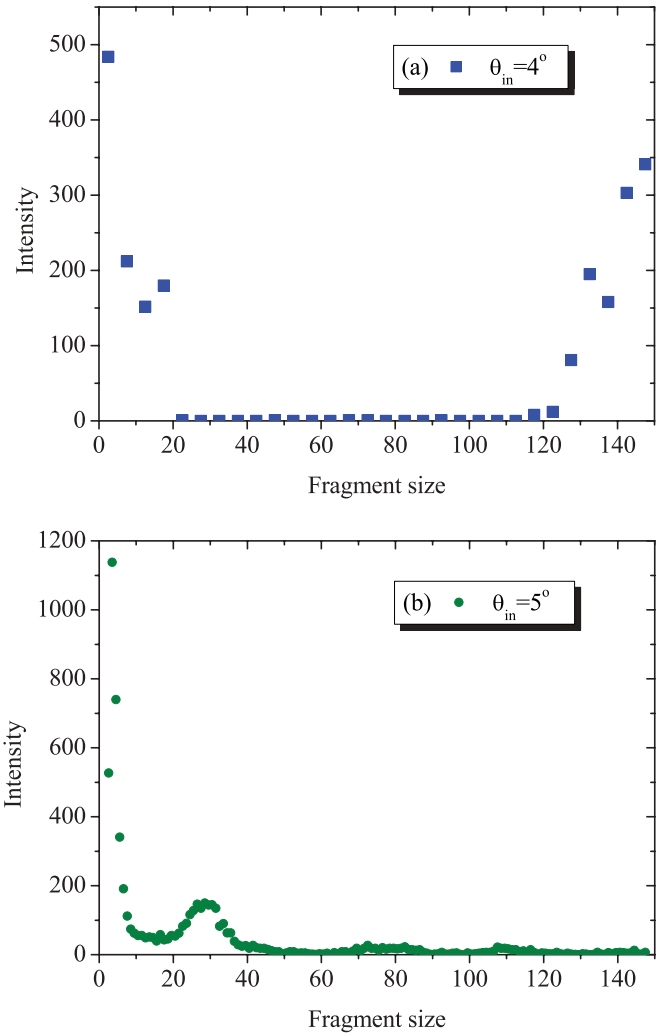

FIG. 6. (Color online) Fragment distributions of 30 keV copper clusters Cu_{147} grazing on a single-crystal Al(111) surface under two incidence angles of $\theta_{in} = 4^\circ,5^\circ$.

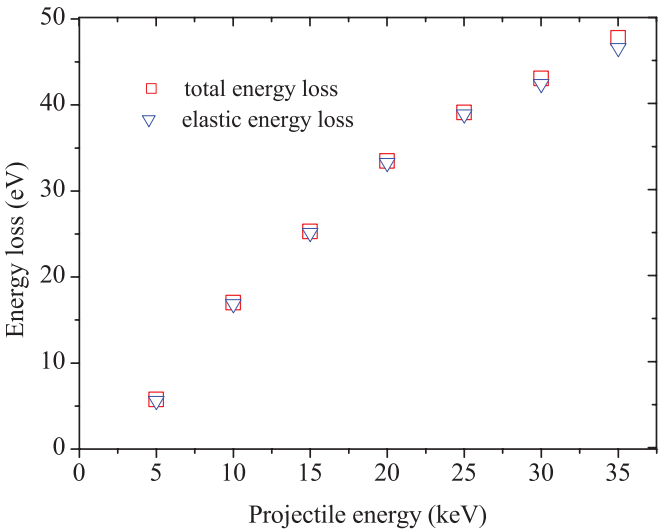

FIG. 7. (Color online) The energy losses as a function of projectile energy for copper clusters Cu_{147} grazing on a single-crystal Al(111) surface under an incident angle of $\theta_{in} = 3^\circ$. Empty square: summation of elastic and inelastic energy loss, i.e., total energy loss. Empty reverse triangle: elastic energy loss. The incident beams graze along random direction $\Phi = 10^\circ$.

Figure 7 shows the energy losses as a function of incident energy for copper clusters Cu_{147} grazing on a single-crystal Al(111) surface under the incident angle of $\theta_{in} = 3^\circ$. As shown above, the total energy loss increases apparently with the increase of cluster energies and nuclear stopping clearly dominates the dissipation of the kinetic energy of projectiles. However, compared to the incident energies, the total energy loss is indeed modest, indicating both nuclear and electronic stopping are strongly suppressed under grazing scattering from the surface.

In the previous work, Hu *et al.* [27] focused their attention on the energy loss of single atomic ions N^{q+} grazing on the Al(111) surface. Their results showed that the total energy loss increases linearly with the incident energy, which is similar to the present observation. However, what is different with Ref. [27] is that the nuclear stopping clearly dominates the stopping process. There is no electronic stopping for incident energies $E = 5,10,15$ keV, because projectiles are still out of the range of surface electron gas. The electronic stopping plays an increasing role with incident energies, but is still at a negligible level even at higher energy ranges. For instance, the distance of closest approach is 4.46 a.u. for incident energy $E = 35$ keV, and the corresponding inelastic energy loss is 1.01 eV, much smaller than the total energy loss of ~48 eV. In addition, since only the largest fragment represents reflected particles, a part of the kinetic energy of projectiles will be taken away by other smaller fragment outcomes. Consequently, the corresponding energy-loss value cannot represent the realistic energy loss caused by traditional nuclear and electronic stopping. Thus, the present energy-loss measurement was done within the energy range at which there is no fragmentation occurring.

Figure 8 shows the energy spectra of reflected particles for 30 keV copper clusters Cu_{147} grazing on a single-crystal Al(111) surface under three different incident angles of $\theta_{in} = 3^\circ,4^\circ,5^\circ$. The main features of the obtained energy spectra can be summarized as follows: For incident angle $\theta_{in} = 3^\circ$, there is only one sharp peak at an energy slightly lower than the incident energy. With the increase of incident angles θ_{in}, the first peak shifts toward lower energies and some additional peaks appear on the left side of the first peak, especially for the angle of incidence $\theta_{in} = 5^\circ$. The first peak shifts toward lower energies due to the fact that the energy loss of the intact reflected Cu_{147} clusters increases with incident angles. This feature is really consistent with the results of Hu *et al.* [27] in which the total energy loss increases significantly if incident angles are larger than 0.9°, provided, e.g., in Fig. 3. In addition, the number and the intensities of these additional peaks increase with incident angles θ_{in}. For instance, compared to $\theta_{in} = 3^\circ$, it is noted that the second, and even the third peak appear for $\theta_{in} = 4^\circ$, indicating that fragmentation of Cu_{147} clusters occurs. Furthermore, the first peak almost disappears and the intensities of the additional peaks are much stronger than that of the first peak for $\theta_{in} = 5^\circ$. This feature is different from the already published work of Matsushita *et al.* [12],

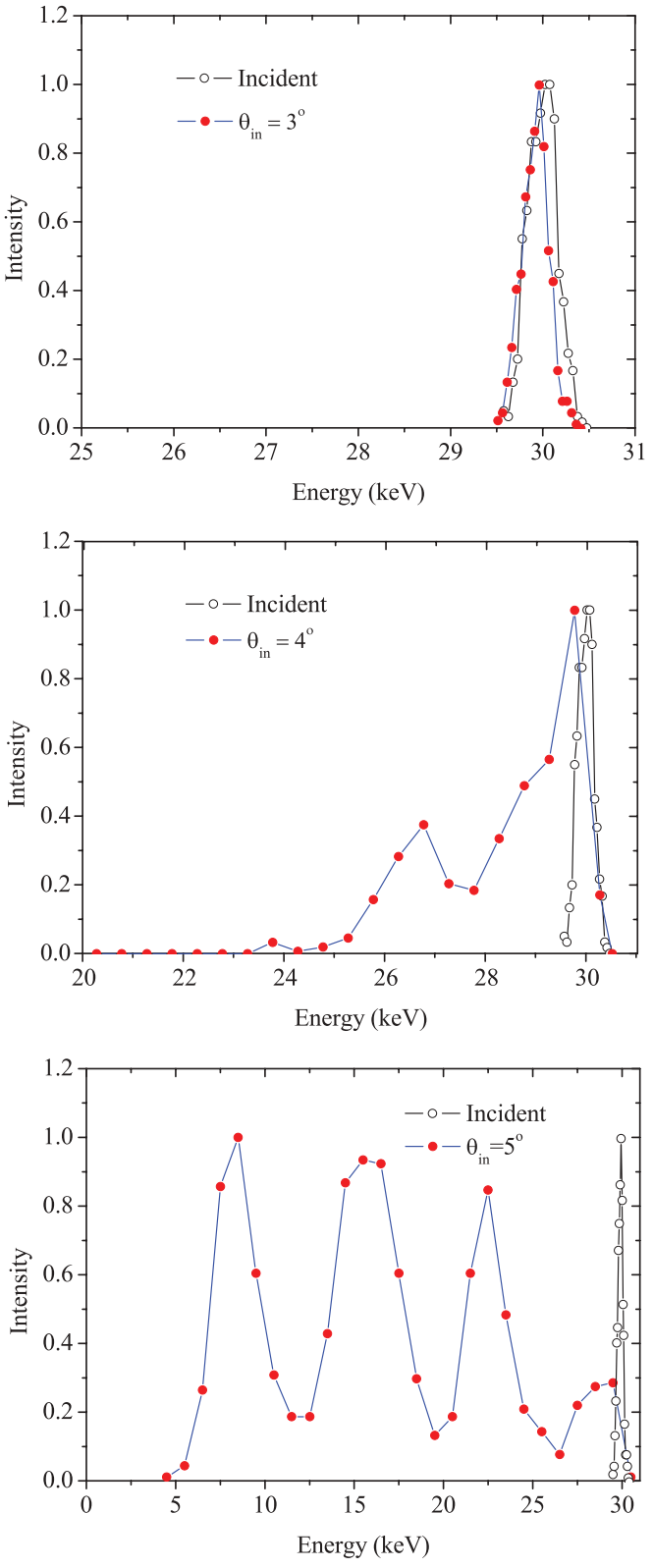

FIG. 8. (Color online) The energy spectra of reflected particles for 30 keV copper clusters Cu_{147} grazing on a single-crystal Al(111) surface under three different incident angles of $\theta_{in} = 3°,4°,5°$.

in which the first peak is obvious and its intensity remains the strongest one with the increase of grazing incidence angles.

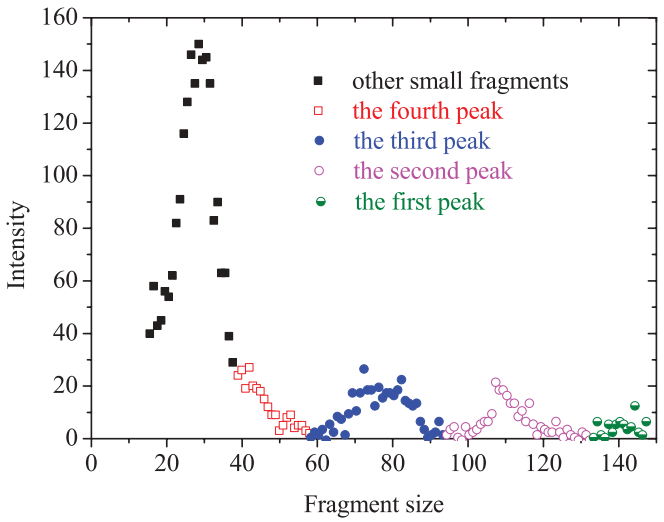

FIG. 9. (Color online) The same as Fig. 6(b), but only the fragments consisting of 15–147 atoms are considered for the fragment distributions of 30 keV copper clusters Cu_{147} grazing scattering from a single-crystal Al(111) surface under angle of incidence $\theta_{in} = 5°$.

According to Fig. 6(b), the intensity of small fragments Cu_n (n = 1–3) is much stronger than that of other fragment outcomes. This feature depends on the fact that almost no intact reflected clusters Cu_{147} can be found after scattering and intensive fragmentation of Cu_{147} clusters happens in each event. Thus, in order to explore detailed information on the reflected fragments Cu_n ($n \geqslant 15$), only the intensity of fragments consisting of 15–147 atoms was shown in Fig. 9. As shown in Fig. 9, there are the first, second, third, and fourth peaks appearing around the fragment size Cu_{144}, Cu_{108}, Cu_{73}, and Cu_{40}, respectively. These specific fragment outcomes can be seen as the clusters dissociation products, which originate from processes that are roughly described by dissociation schemes as follows: (i) The fragment Cu_{144} originated from $Cu_{147} \rightarrow Cu_n(n = 1-3) + \cdots + Cu_{144}$, leading to strong intensity of small fragments Cu_n (n = 1–3). (ii) The fragment Cu_{144} will undergo further fragmentation $Cu_{144} - k^*Cu_{35}(k = 1,2,3) - Cu_s - Cu_m \cdots \cdots \rightarrow Cu_n$ (n = 108,73,40), where Cu_s and Cu_m stand for other small fragments with random size. Since fragment Cu_{144} will undergo further fragmentation, the intensity of the first peak associated with fragment Cu_{144} is weak. For instance, fragment Cu_{108} originates from $Cu_{144} - Cu_{35} - Cu_1 \rightarrow Cu_{108}$, whereas dissociation scheme $Cu_{144} - 3^*Cu_{35} - Cu_m$ (m = 1–39) $\rightarrow Cu_{40}$ is accompanied by small fragments Cu_m (m = 1–39), leading to strong intensity of small fragments marked as black solid squares in Fig. 9.

In the work of Matsushita *et al.* [12], if the collision energy of a C_{60}^+ ion impacting on a solid surface is larger than but not far beyond the threshold energy, fragmentation of C_{60}^+ would occur via a sequential C_2-loss process. A similar mechanism has been mentioned by Beck *et al.* [28] who studied several fullerenes within the energy range from 150 to 1050 eV. They concluded that at energies near fragmentation threshold, the fragmentation will involve the ejection of C_2 units, but that at higher impact energies, the fullerene seems to

undergo further fragmentation, resulting in a large number of smaller fragments. In the present work, regarding the incident angle $\theta_{in} = 5^\circ$, the vertical energy $E_\perp$ is 227.88 eV, which is much beyond the critical energy, and the percentage of clusters that remain unfragmented can even go down to 0.4. Intensive fragmentation of Cu_{147} clusters occurs, and therefore the possibility of detecting the intact outgoing Cu_{147} clusters is really small. Furthermore, the observed peaks are almost equally separated by ∼7.0 keV for incident angle $\theta_{in} = 5^\circ$, which is in agreement with the kinetic energy carried by fragment Cu_{35}, i.e., ∼35/147 of the kinetic energy of Cu_{147}, being ∼7.14 keV. The feature indicates that the fragmentation of Cu_{147} occurs via successive "knockouts" of small fragments in large-angle cluster-surface grazing scattering.

A structureless wall and efficient program were used in the work of Chancey *et al*. [11], promising them to perform simulation with a modest consumption of computer resources. However, the structureless wall lacks an atomic structure. Their results show that there is a threshold impact energy of ∼150 eV for fragmentation of C_{60}, i.e., the threshold energy is 2.5 eV/atom. The threshold energy is much smaller than the binding energy of C_{60}, ∼7.6 eV. Consequently, the ratio of threshold energy to binding energy for C_{60} is 0.32. In our work, the single-crystal Al(111) target with accurate surface channels was used. The threshold vertical energy for the fragmentation of Cu_{147} is ∼0.884 eV/atom, and is also smaller than the binding energy of Cu_{147}, ∼3.388 eV/atom. The copper clusters appear more easily to dissociate into fragments, compared to C_{60}. In addition, the ratio of threshold energy to binding energy for Cu_{147} is 0.26, and therefore, this qualitative result is not sensitive to the details of the descriptions of lattice surface even if there is a lack of atomic structure or the details of surface structure description.

IV. CONCLUSION

A molecular dynamics simulation study of the interaction for copper clusters Cu_n grazing scattering from a single-crystal Al(111) surface has been presented. The screened Coulomb potential and tight-binding potential are used to model the motion of clusters. The copper clusters Cu_n with energies from which no fragmentation occurs to those producing intensive atomization serve as projectiles. We have found that the percentage of clusters that remain unfragmented depends significantly on incident energies, incident angles, and incident cluster sizes. However, the surface structure almost has no influence on cluster-surface interaction with respect to the fragmentation process. Additionally, the clusters without icosahedral structure appear to be less stable. The multipeak structures of the obtained energy spectra were found for large angle of incidence $\theta_{in} = 5^\circ$, indicating the successive knockouts feature of small fragments occurs in cluster-surface grazing scattering.

ACKNOWLEDGMENTS

This work was supported by National Natural Science Foundation of China under Grants No. 11135002, No. 11075069, No. 91026021, No. 11075068, and No. 10975065, and the Fundamental Research Funds for the Central Universities with Grant No. lzujbky-2010-k08. Moreover, the authors would like to thank lecturer Xiaodong Pan and Dr. Hongchuan Du for valuable suggestions and discussions on the building of copper clusters geometry.

[1] Thomas Kunert and Rüdiger Schmidt, Phys. Rev. Lett. **86**, 5258 (2010).
[2] Şakir Erkoç and Riad Shaltaf, Phys. Rev. A **60**, 3053 (2003).
[3] F. J. Resende and B. V. Costa, Surf. Sci. **481**, 54 (2001).
[4] Jian-Hua Zhang, Yang Zhang, Yu-Hua Wen, and Zi-Zhong Zhu, Comput. Mater. Sci. **48**, 250 (2010).
[5] N. Neumann, D. Hant, L. Ph. H. Schmidt, J. Titze, T. Jahnke, A. Czasch, M. S. Schöffler, K. Kreidi, O. Jagutzki, H. Schmidt-Böcking, and R. Dörner, Phys. Rev. Lett. **104**, 103201 (2010).
[6] A. Kaplan, A. Bekkerman, E. Gordon, B. Tsipinyuk, M. Fleischer, and E. Kolodney, Nucl. Instrum. Methods Phys. Res. B **232**, 184 (1999).
[7] S. Wethekam, H. Winter, H. Cederquist, and H. Zettergren, Phys. Rev. Lett. **99**, 037601 (2007).
[8] S. Wethekam, A. Schüller, and H. Winter, Nucl. Instrum. Methods Phys. Res. B **258**, 68 (1999).
[9] A. Mertens and H. Winter, Phys. Rev. Lett. **85**, 2825 (2000).
[10] K. Kimura, T. Matsushita, K. Nakajima, and M. Suzuki, Nucl. Instrum. Methods Phys. Res. B **267**, 2638 (1999).
[11] Ryan T. Chancey, Lene Oddershede, Frank E. Harris, and John R. Sabin, Phys. Rev. A **67**, 043203 (2003).
[12] Y. Susuki, M. Fritz, K. Kimura, M. Mannami, N. Sakamoto, H. Ogawa, I. Katayama, T. Noro, and H. Ikegami, Phys. Rev. A **51**, 3868 (1995).
[13] T. Matsushita, K. Nakajima, M. Suzuki, and K. Kimura, Phys. Rev. A **76**, 032903 (2007).
[14] Fabrizio Cleri and Vittorio Rosato, Phys. Rev. B **48**, 22 (1993).
[15] Giorgio Mazzone, Vittorio Rosato, Marco Pintore, Francesco Delogu, PierFranco Demontis, and Giuseppe B. Suffritti, Phys. Rev. B **55**, 837 (1996).
[16] C. C. Hwang, J. G. Chang, G. J. Huang, and S. H. Huang, J. Appl. Phys. **92**, 5904 (2002).
[17] Z. H. Hong, S. F. Hwang, and T. H. Fang, J. Appl. Phys. **103**, 124313 (2008).
[18] N. Levanov, V. S. Stepanyuk, W. Hergert, O. S. Trushin, and K. Kokko, Surf. Sci. **400**, 54 (1998).
[19] H. Winter, Phys. Rep. **367**, 387 (2002).
[20] Mukul Kabir, Abhijt Mookerjee, and A. K. Bhattacharya, Phys. Rev. A **69**, 043203 (2004).
[21] Valeri G. Grigoryan, Denitsa Alamanova, and Michael Springborg, Phys. Rev. B **73**, 115415 (2006).
[22] Xianwen Luo, Bitao Hu, Chengjun Zhang, Jijin Wang, and Chunhua Chen, Phys. Rev. A **81**, 052902 (2010).
[23] W. Huang, H. Lebius, R. Schuch, M. Grether, and N. Stolterfoht, Phys. Rev. A **58**, 2962 (1998).
[24] Yuan-Hong Song, You-Nian Wang, and Z. L. Miskovic, Phys. Rev. A **63**, 052902 (2001).
[25] W. Brandt and M. Kitagawa, Phys. Rev. B **25**, 5631 (1982).

[26] Y. N. Wang and W. -K. Liu, Phys. Rev. A **54**, 636 (1996).
[27] Hu Bi-Tao, Chen Chun-Hua, Song Yu-Shou, and Gu Jian-Gang, Chin. Phys. Soc. **16**, 1009 (2007).
[28] R. D. Beck, J. Rockenberger, P. Weis, and M. M. Kappes, J. Chem. Phys. **104**, 3638 (1996).
[29] B. Concina, S. Tomita, J. U. Anderson, and P. Hvelplund, Eur. Phys. J. D **34**, 191 (2005).
[30] S. Wethekam and H. Winter, Phys. Rev. A **76**, 032901 (2007).
[31] S. Wethekam, J. Merck, M. Busch, and H. Winter, Phys. Rev. B **83**, 085423 (2011).